Journal of Organometallic Chemistry 695 (2010) 1337–1345

Contents lists available at ScienceDirect

Journal of Organometallic Chemistry

journal homepage: www.elsevier.com/locate/jorganchem

Ethynylmonocarba-*closo*-dodecaborates: M[12-HCC-*closo*-1-$CB_{11}H_{11}$] and M[7,12-$(HCC)_2$-*closo*-1-$CB_{11}H_{10}$] (M = Cs^+, $[Et_4N]^+$)

Alexander Himmelspach, Maik Finze *

Institut für Anorganische Chemie und Strukturchemie II, Heinrich-Heine-Universität Düsseldorf, Universitätsstraße 1, 40225 Düsseldorf, Germany

ARTICLE INFO

Article history:
Received 29 October 2009
Received in revised form 9 February 2010
Accepted 13 February 2010
Available online 19 February 2010

Keywords:
Monocarba-*closo*-dodecaborates
Alkynes
Boron
NMR spectroscopy
Structure elucidation

ABSTRACT

Cesium and tetraethylammonium salts of the ethynyl functionalized monocarba-*closo*-dodecaborate anions [12-HCC-*closo*-1-$CB_{11}H_{11}]^-$ and [7,12-$(HCC)_2$-*closo*-1-$CB_{11}H_{10}]^-$ were obtained by desilylation of $[Et_4N]$[12-Me_3SiCC-*closo*-1-$CB_{11}H_{11}$] and $[Et_4N]$[7,12-$(Me_3SiCC)_2$-*closo*-1-$CB_{11}H_{10}$], respectively. Their thermal properties were examined by differential scanning calorimetry. The compounds were characterized by multi-NMR, IR, and Raman spectroscopy, (−)-MALDI mass spectrometry, and elemental analysis. Single-crystals of Cs[12-HCC-*closo*-1-$CB_{11}H_{11}$] and $[Et_4N]$[7,12-$(HCC)_2$-*closo*-1-$CB_{11}H_{10}$] were studied by X-ray diffraction. The discussion of the spectroscopic and structural properties is supported by data derived from theoretical calculations using density functional theory as well as perturbation theory.

1. Introduction

Functionalized monocarba-*closo*-dodecaborate anions are used as building blocks in a variety of applications [1–5], for example in ionic liquids [6,7] catalysis [8–15], pharmaceuticals [16,17] and polymers [18,19]. A consequence of the constantly growing demand for functionalized monocarba-*closo*-dodecaborate anions is the increasing search for efficient procedures for the derivatization of the {*closo*-1-CB_{11}} cage [1–5]. In contrast to substitution reactions at the carbon vertex of the {*closo*-1-CB_{11}} cluster that are well developed, the selective introduction of a functional group that can be modified easily at one of the boron vertices is less studied [1]. A strategy for the functionalization at the antipodal boron atom and the upper belt boron atoms of the {*closo*-1-CB_{11}} cluster is the partial iodination followed by exchange of the iodine substituent(s) against an alkyl [20], aryl [20–22] allyl [23,24], or alkynyl [25] group(s) by Pd-catalyzed cross-coupling reactions, that was first introduced into boron cluster chemistry for the related neutral dicarba-*closo*-dodecaboranes in the early 1980s [26–28].

Recently, we have reported on the preparation of first examples of salts of phenylalkynyl and trimethylsilylalkynyl substituted monocarba-*closo*-dodecaborate anions via Pd-catalyzed Kumada-type [29,30] cross-coupling reactions [25]. {*closo*-1-CB_{11}} clusters with alkynyl substituents bonded to the boron atom in the antipodal position (B12) or to one of the boron atoms of the upper B_5 belt (B7) have been obtained. Mono- and diiodinated monocarba-*closo*-dodecaborate anions that are accessible by iodination of the [*closo*-1-$CB_{11}H_{12}]^-$ anion or of its derivatives [20,31,32] are the starting materials for these cross-coupling reactions with alkynyl Grignard reagents. In Scheme 1 the two-step syntheses of the anions [12-Me_3SiCC-*closo*-1-$CB_{11}H_{11}]^-$ and [7,12-$(Me_3SiCC)_2$-*closo*-1-$CB_{11}H_{10}]^-$ starting from [*closo*-1-$CB_{11}H_{12}]^-$ are depicted [25].

In this paper we report on the syntheses and thermal properties of the cesium and tetraethylammonium salts of the ethynyl functionalized monocarba-*closo*-dodecaborate anions [12-HCC-*closo*-1-$CB_{11}H_{11}]^-$ (**1**) and [7,12-$(HCC)_2$-*closo*-1-$CB_{11}H_{10}]^-$ (**2**). The multi-NMR and vibrational spectroscopic characterization is aided by data derived from theoretical calculations. Furthermore, the crystal structures of Cs[12-HCC-*closo*-1-$CB_{11}H_{11}$] (Cs-**1**) and $[Et_4N]$[7,12-$(HCC)_2$-*closo*-1-$CB_{11}H_{10}$]($[Et_4N]$-**2**) are presented.

2. Experimental

2.1. General

Reactions involving air-sensitive compounds were performed under argon using standard Schlenk line techniques. ^1H, ^{11}B, and ^{13}C NMR spectra were recorded at room temperature, either in $(CD_3)_2CO$ or in CD_3CN on a Bruker Avance III 400 spectrometer operating at 400.17, 100.62, and 128.39 MHz for ^1H, ^{13}C, and ^{11}B nuclei, respectively. NMR signals were referenced against TMS (^1H, ^{13}C) and $BF_3{\cdot}OEt_2$ in CD_3CN (^{11}B) as external standards. Infrared and Raman spectra were recorded at room temperature on an Excalibur FTS 3500 spectrometer (Digilab, Germany) with an

* Corresponding author. Tel.: +49 211 81 13144; fax: +49 211 81 14146.
E-mail address: maik.finze@uni-duesseldorf.de (M. Finze).

0022-328X/$ - see front matter © 2010 Elsevier B.V. All rights reserved.
doi:10.1016/j.jorganchem.2010.02.011

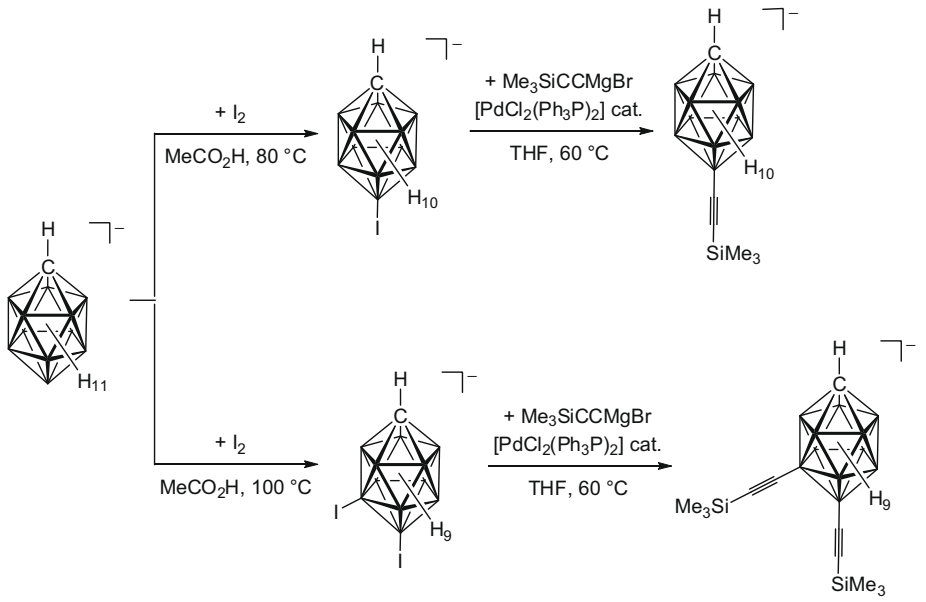

Scheme 1. Synthesis of the anions [12-Me_3SiCC-*closo*-1-$CB_{11}H_{11}$]$^-$ and [7,12-$(Me_3SiCC)_2$-*closo*-1-$CB_{11}H_{10}$]$^-$ starting from the [*closo*-1-$CB_{11}H_{12}$]$^-$ anion [25].

apodized resolution of 2 cm^{-1} (IR) and 2–4 cm^{-1} (Raman), respectively. IR spectra were measured in the attenuated total reflection (ATR) mode in the region of 4000–530 cm^{-1}. Raman spectra were measured using the 1064 nm excitation line of a Nd/YAG laser on crystalline samples contained in melting point capillaries in the region of 3500–80 cm^{-1}. Matrix-assisted laser desorption/ionization (MALDI) mass spectra in the negative-ion mode were recorded on a Bruker Ultraflex TOF spectrometer. Thermo-analytical measurements were made with a Mettler Toledo DSC 30 instrument in the temperature range of 25–600 °C. About 2–6 mg of the solid samples were weighed and contained in sealed aluminum crucibles. The studies were performed with a heating rate of 5 K min^{-1}; throughout this process the furnace was flushed with dry N_2. Elemental analysis (C, H, N) were performed with a Euro EA3000 instrument (HEKA-Tech, Germany).

2.2. Chemicals

All standard chemicals were obtained from commercial sources. [Et_4N][12-Me_3SiCC-*closo*-1-$CB_{11}H_{11}$] [25] and [Et_4N][7,12-$(Me_3SiCC)_2$-*closo*-1-$CB_{11}H_{10}$] [25] were prepared as described in the literature from the corresponding iodinated monocarba-*closo*-dodecaborates Cs[12-I-*closo*-1-$CB_{11}H_{11}$] [20,31] and Cs[7,12-I_2-*closo*-1-$CB_{11}H_{10}$] [31] and $Me_3SiCCMgBr$ via Kumada-type cross-coupling reactions.

2.3. [Et_4N][12-HCC-closo-1-$CB_{11}H_{11}$]([Et_4N]-**1**)

[Et_4N][12-Me_3SiCC-*closo*-1-$CB_{11}H_{11}$] (550 mg, 1.49 mmol) was dissolved in a solution of potassium hydroxide in ethanol (10 mL, 1.5 mol L^{-1}) and stirred at room temperature for three hours. While stirring 100 mL of water were added resulting in the formation of a precipitate. The colorless salt [Et_4N]-**1** was filtered off and dried in vacuum. Yield: 428 mg (1.44 mmol, 97%). Anal. Calc. for $C_{11}H_{32}B_{11}N$ (297.305 g mol^{-1}): C, 44.44; H, 10.85; N, 4.71. Found: C, 44.02; H, 10.32; N, 4.56%. MS (MALDI) negative, *m/z* (isotopic abundance): Calc. for **1** ($[C_3H_{12}B_{11}]^-$): 163(3), 164(13), 165(37), 166(74), 167(100), 168(82), 169(32), 170(1). Found: 162(<1), 163(<1), 164(11), 165(32), 166(63), 167(100), 168(72), 169(31), 170(<1).

2.4. [Et_4N][7,12-$(HCC)_2$-closo-1-$CB_{11}H_{10}$]([Et_4N]-**2**)

The desilylation of [Et_4N][7,12-$(Me_3SiCC)_2$-*closo*-1-$CB_{11}H_{10}$] was performed as described for the synthesis of [Et_4N]-**1**. [Et_4N]-**2** was isolated as a white solid. Yield: 325 mg (1.01 mmol, 95%). Anal. Calc. for $C_{13}H_{32}B_{11}N$ (321.327 g mol^{-1}): C, 48.59; H, 10.04; N, 4.36. Found: C, 48.14; H, 9.65; N, 4.51%. MS (MALDI) negative, *m/z* (isotopic abundance): Calc. for **2** ($[C_5H_{12}B_{11}]^-$): 187(3), 188(13), 189(37), 190(74), 191(100), 192(83), 193(33), 194(2). Found: 187(1), 188(12), 189(39), 190(76), 191(100), 192(85), 193(36), 194(2).

2.5. Cs[12-HCC-closo-1-$CB_{11}H_{11}$](Cs-**1**)

[Et_4N]-**1** (360 mg, 1.21 mmol) was suspended in aqueous HCl (10 mL, 5% v/v), and extracted with Et_2O (3 × 40 mL). The combined ethereal layers were dried with $MgSO_4$ and filtered. An aqueous solution of Cs_2CO_3 (400 mg, 1.23 mmol, 5 mL) was added to the diethyl ether solution. The solvents were removed using a rotary evaporator and the solid residue was extracted with acetone (2 × 50 mL), dried with Cs_2CO_3 and most of the acetone was removed under reduced pressure. Addition of chloroform resulted in the immediate formation of an off-white solid that was isolated via filtration. Cs-**1** was dried overnight in a high vacuum. Yield: 333 mg (1.11 mmol, 92%). Anal. Calc. for $C_3H_{12}B_{11}Cs$ (299.950 g mol^{-1}): C, 12.01; H, 4.03. Found: C, 11.60; H, 3.72%.

2.6. Cs[7,12-$(HCC)_2$-closo-1-$CB_{11}H_{10}$](Cs-**2**)

Cs-**2** was obtained as an off-white solid starting from [Et_4N]-**2** following the protocol described for the preparation of Cs-**1**. Yield: 350 mg (1.08 mmol, 93%). Anal. Calc. for $C_5H_{12}B_{11}Cs$ (323.972 g mol^{-1}): C, 18.54; H, 3.73. Found: C, 18.21; H, 3.51%.

2.7. Single-crystal X-ray diffraction

Concentrated solutions of the salts Cs[12-HCC-*closo*-1-$CB_{11}H_{11}$] (Cs-**1**) and [Et_4N][7,12-$(HCC)_2$-*closo*-1-$CB_{11}H_{10}$]([Et_4N]-**2**) in acetonitrile were filled into vials that were placed into flasks partially filled with chloroform. After a few days colorless crystals of Cs-**1** and [Et_4N]-**2** suitable for X-ray diffraction were obtained at room

temperature. A crystal of Cs-**1** was studied using an imaging plate diffraction system (IPDS, Stoe & Cie) at 123 K and a crystal of [Et_4N]-**2** was investigated with a CCD diffractometer (STADI CCD, Stoe & Cie) at 293 K using Mo Kα radiation (λ = 0.71073 Å), respectively. Numerical absorption corrections [33] based on indexed crystal faces were applied to the data of Cs-**1** after optimization of the crystal shape [34]. All structures were solved by direct methods [35,36], and refinement is based on full-matrix least-squares calculations on F^2 [36,37].

Cs[12-HCC-*closo*-1-$CB_{11}H_{11}$] (Cs-**1**) crystallizes in the monoclinic space group $P2_1/n$ and the crystal contains a small amount of Cs[12-I-*closo*-1-$CB_{11}H_{11}$]. The batch of Cs-**1** used for the crystallization was obtained from an incomplete cross-coupling reaction of the [12-I-*closo*-1-$CB_{11}H_{11}$]$^-$ anion with $Me_3SiCCMgBr$ [25]. According to $^{11}B\{1H\}$ NMR spectroscopy the content of Cs[12-I-*closo*-1-$CB_{11}H_{11}$] of the substance used for the crystallization was 5%. In the crystal the anions **1** and [12-I-*closo*-1-$CB_{11}H_{11}$]$^-$ are disordered and the ethynyl group and the iodine substituent are superimposed. Related cocrystallizations are well documented and examples with boron clusters have been reported, as well [38]. During the refinement of the occupancies, which resulted in 94% of **1** and 6% of [12-I-*closo*-1-$CB_{11}H_{11}$]$^-$, the atoms of the ethynyl group and the iodine atom were treated isotropically. While keeping these refined occupancies fixed, all non-hydrogen atoms were refined anisotropically without applying any restraints. All hydrogen atoms were located in electron-density difference maps. The hydrogen atoms bonded to the atoms of the {*closo*-CB_{11}} cage were allowed to ride on the coordinates of the parent boron and carbon atom and their isotropic displacement parameters were kept equal to 130% of the U_{eq} of the respective parent atom. The acetylenic hydrogen atom was placed in a calculated position and the isotropic displacement parameter was fixed at 140% of the U_{eq} of the associated carbon atom of the ethynyl group.

The tetraethylammonium salt of the [7,12-$(HCC)_2$-*closo*-1-$CB_{11}H_{10}$]$^-$ anion ([Et_4N]-**2**) crystallizes in the orthorhombic space group *Pnma*. The anion **2** is located on a mirror plane resulting in a disordering over two positions with equal occupancies. Anisotropic displacement parameters were applied to all of the atoms heavier than hydrogen. All hydrogen atoms were located in electron-density difference maps but replaced in calculated positions. The isotropic displacement parameters of the hydrogen atoms were fixed to U_{eq} of the respective parent atom at 130% for the hydrogen atoms bonded to the cluster boron and carbon atoms and at 150% for the hydrogen atom of the ethynyl group and the hydrogen atoms of the ethyl groups of the [Et_4N]$^+$ cation.

Most of the calculations were carried out using the WINGX program package [39]. The molecular structure diagrams were drawn with the program DIAMOND 3.2c [40]. Experimental details and crystal data are collected in Table 1.

2.8. Quantum chemical calculations

Density functional calculations (DFT) [41] were carried out using Becke's three-parameter hybrid functional and the Lee-Yang-Parr correlation functional (B3LYP) [42–44] using the GAUSSIAN03 program suite [45]. Geometries were optimized, and energies were calculated with the 6-311++G(d,p) basis sets. Diffuse functions were incorporated because improved energies are obtained for anions [46]. All structures represent true minima with no imaginary frequency on the respective hypersurface. In addition, the geometries were optimized at the second-order Møller-Plesset perturbation (MP2) level of theory, using the resolution-of-the-identity approximation [(RI)-CC2 module] [47]) in combination with the def2-TZVPP basis sets and auxiliary bases [48].

DFT-GIAO [49] NMR shielding constants $\sigma(^1H)$, $\sigma(^{11}B)$ and $\sigma(^{13}C)$ as well as spin-spin coupling constants [50–53] were calculated at the B3LYP/6-311++G(2d,p) level of theory using the geometries computed at the B3LYP/6-311++G(d,p) level of theory with the Gaussian03 program suite [45]. The ^1H, ^{11}B, and ^{13}C NMR shielding constants were calibrated to the respective chemical shift scale $\delta(^1H)$, $\delta(^{11}B)$, and $\delta(^{13}C)$ using predictions on diborane(6) and Me_4Si with chemical shifts of −16.6 ppm for B_2H_6 [54] ($\delta(^{11}B)$) and 0 ppm for Me_4Si ($\delta(^1H)$ and $\delta(^{13}C)$) [55].

Table 1
Crystallographic data of Cs[12-HCC-*closo*-1-$CB_{11}H_{11}$][a] (Cs-**1**) and [Et_4N][7,12-$(HCC)_2$-*closo*-1-$CB_{11}H_{10}$] ([Et_4N]-**2**).

	Cs-**1**[a]	[Et_4N]-**2**
Chemical formula	$C_{2.88}H_{11.94}B_{11}CsI_{0.06}$[a]	$C_{13}H_{32}B_{11}N_1$
Formula weight (g mol^{-1})	306.067	321.327
T (K)	123	293
Color	Colorless	Colorless
Crystal size (mm^3)	0.10 × 0.10 × 0.08	0.15 × 0.12 × 0.07
Crystal system, space group	Monoclinic, $P2_1/n$	Orthorhombic, *Pnma*
a (Å)	12.5020(9)	14.030(5)
b (Å)	6.7990(4)	11.000(4)
c (Å)	13.9820(12)	13.288(5)
β (°)	98.609(9)	
Volume (Å^3)	1171.641(15)	2050.7(13)
Z	4	4
D_{calc} (Mg m^{-3})	1.735	1.041
Absorption coefficient (mm^{-1})	3.263	0.051
F(0 0 0) (e)	570	688
θ Range (°)	2.04–24.98	4.22–24.15
Reflections collected/unique	9085/2035	27179/1723
R_{int} (%)	6.73	8.50
Data/restraints/parameters	2035/0/156	1723/0/124
R_1 ($I > 2\sigma(I)$)[b]	0.0284	0.0799
wR_2 (all)[c]	0.0690	0.1453
Goodness-of-fit (GOF_ on F^2[d]	1.073	1.145
Largest difference in peak/hole (e Å^{-3})	1.315/−0.401	0.191/−0.160

[a] Contains 6% of Cs[12-I-*closo*-1-$CB_{11}H_{11}$].
[b] $R_1 = (\sum||F_o| - |F_c||)/\sum|F_o|$.
[c] $wR_2 = [\sum w(F_o^2 - F_c^2)^2/\sum w(F_o^2)^2]^{0.5}$, weight scheme: $w = [\sigma^2F_o + (aP)^2 + bP]^{-1}$; $P = [\max(0,F_o^2) + 2F_c^2]/3$; Cs-**1**: a = 0.0282, b = 1.8230; [Et_4N]-**2**: a = 0.0249, b = 1.8124.
[d] GOF: $S = \sum w(F_o^2 - F_c^2)^2/(m - n)$; ($m$ = reflections, n = variables).

3. Results and discussion

3.1. Synthetic aspects

In basic ethanol solution the trimethylsilylalkynyl substituted monocarba-*closo*-dodecaborate anions [12-Me_3SiCC-*closo*-1-$CB_{11}H_{11}$]$^-$ and [7,12-$(Me_3SiCC)_2$-*closo*-1-$CB_{11}H_{10}$]$^-$ were desilylated to result in the anions [12-HCC-*closo*-1-$CB_{11}H_{11}$]$^-$ (**1**) and [7,12-$(HCC)_2$-*closo*-1-$CB_{11}H_{10}$]$^-$ (**2**), respectively (Scheme 2). The tetraethylammonium salts of **1** and **2** were isolated in yields of approximately 96% by precipitation from the reaction mixtures upon addition of water.

The [Et_4N]$^+$ salts were transformed into the corresponding cesium salts via an extraction protocol: the tetraethylammonium salts were suspended in aqueous HCl and the anions were extracted into diethyl ether as [$H(OEt_2)_n$]$^+$ salts. Addition of aqueous Cs_2CO_3 to the ethereal phases yielded the Cs^+ salts of **1** and **2**.

The four cesium and tetraethylammonium salts exhibit high thermal stabilities and their decomposition starts at 205 °C for [Et_4N]-**1**, 265 °C for Cs-**1**, 289 °C for [Et_4N]-**2**, and 210 °C for Cs-**2**.

3.2. Single-crystal structures

Cs[12-HCC-*closo*-1-$CB_{11}H_{11}$] (Cs-**1**) crystallizes in the monoclinic space group $P2_1/n$ (no. 14) with four formula units in the unit cell (Fig. 1 and Table 2). Since the batch of Cs-**1** that was used for

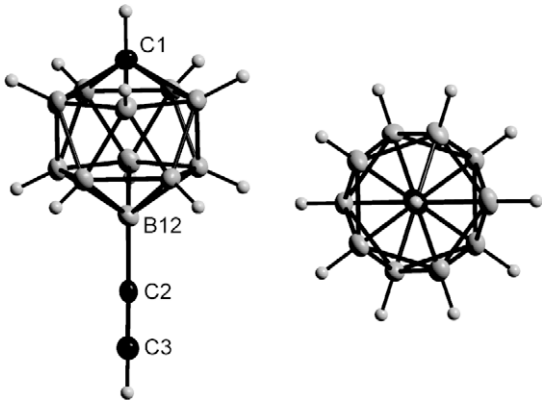

Fig. 1. Two different views of the [12-HCC-*closo*-$CB_{11}H_{11}$]$^-$ anion in the crystal structure of Cs-**1** (displacement ellipsoids at the 50% probability level).

the crystallization was obtained from an incomplete synthesis of [Et_4N][12-Me_3SiCC-*closo*-1-$CB_{11}H_{11}$] [25] (95% conversion) the crystal studied contained a small amount of Cs[12-I-*closo*-1-$CB_{11}H_{11}$]. Refinement of the occupancies resulted in 6% of Cs[12-I-*closo*-1-$CB_{11}H_{11}$]. The anions **1** and [12-I-*closo*-1-$CB_{11}H_{11}$]$^-$ are disordered and the positions of the ethynyl substituent and the iodine atom are superimposed. The structure was refined without restraints and the influence on the interatomic distances and angles determined is small (Table 2). For the [12-I-*closo*-1-$CB_{11}H_{11}$]$^-$ anion in the crystal of Cs-**1** a *d*(B–I) of 2.172(9) Å was found that compares well to other boron–iodine bond lengths in monocarba-*closo*-dodecaborate derivatives, for example 2.196(6) Å in 1-R-12-I-*closo*-1-$CB_{11}H_{10}$ (R = 4-pentylquinuclidin-1-yl) [56] and 2.19(1) Å in [7-I-12-HO-*closo*-1-$CB_{11}H_{10}$]$^-$ [32].

[Et_4N][7,12-$(HCC)_2$-*closo*-1-$CB_{11}H_{10}$] ([Et_4N]-**2**) crystallizes in the orthorhombic space group *Pnma* (no. 62) with $Z = 4$. The [7,12-$(HCC)_2$-*closo*-1-$CB_{11}H_{10}$]$^-$ anion (**2**) is located on a crystallographic mirror plane and it is disordered over two positions (Fig. 2). Hence, the experimentally determined interatomic distances are averaged values for the two different ethynyl groups and the {*closo*-1-CB_{11}} cluster in anion **2**. Due to the disorder the quality of the interatomic distances derived from the crystal structure analysis of [Et_4N]-**2** is relatively low (Table 2).

The most relevant properties of the anions [12-HCC-*closo*-1-$CB_{11}H_{11}$]$^-$ (**1**) and [7,12-$(HCC)_2$-*closo*-1-$CB_{11}H_{10}$]$^-$ (**2**) are summarized in Table 2 and compared to values derived from *ab initio* calculations at the (RI)-MP2/def2-TZVPP level of theory (Fig. 3) and from DFT calculations at the B3LYP/6-311++G(d,p) level of theory. The bond lengths and angles calculated for **1** using the two different theoretical methods are in good agreement and they compare well to the experimentally determined values of Cs-**1**. The results of the different theoretical calculations performed for anion **2** are very similar as well, however, the experimental bonding properties exhibit strong deviations compared to their theoretical counterparts which is most probably a result of the disorder of the anion in the structure of [Et_4N]-**2**.

The interatomic distances and angles of [12-HCC-*closo*-1-$CB_{11}H_{11}$]$^-$ (**1**) in its Cs^+ salt are close to the corresponding values reported for the related [12-PhCC-*closo*-1-$CB_{11}H_{11}$]$^-$ anion in the [Et_4N]$^+$ salt [57]: the alkynyl fragments are nearly linear and the B–C and C≡C distances are *d*(B–C) = 1.568(8) Å and *d*(C≡C) =

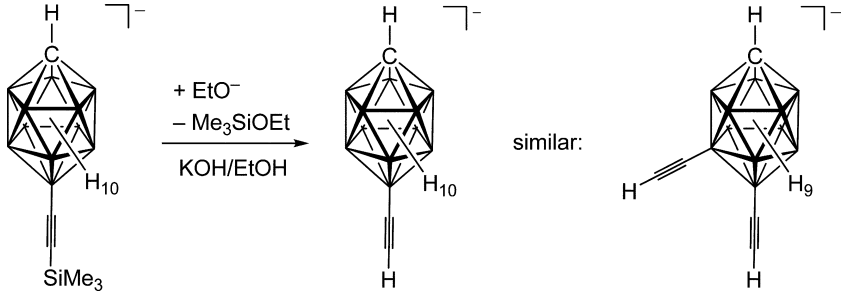

Scheme 2. Desilylation reactions of {*closo*-1-CB_{11}} clusters with trimethylsilylalkynyl substituents.

Table 2
Experimental and calculated[a,b] bond lengths and angles of [12-HCC-*closo*-1-$CB_{11}H_{11}$]$^-$ (**1**) and [7,12-$(HCC)_2$-*closo*-1-$CB_{11}H_{10}$]$^-$ (**2**).

	[12-HCC-*closo*-1-$CB_{11}H_{11}$]$^-$ (**1**)			[7,12-$(HCC)_2$-*closo*-1-$CB_{11}H_{10}$]$^-$ (**2**)		
	Cs^+ salt	(RI)-MP2[a]	B3LYP[b]	[Et_4N]$^+$ salt	(RI)-MP2[a]	B3LYP[b]
Symmetry	C_1	C_{5v}	C_{5v}	(C_s)[c]	C_s	C_s
Bond lengths [Å]						
C≡C (B12)	1.172(10)	1.222	1.211	1.01(2)	1.222	1.210
C≡C (B7)	–	–	–	1.01(2)	1.222	1.210
B–C (B12)	1.568(8)	1.534	1.545	1.62(3)	1.530	1.542
B–C (B7)	–	–	–	1.62(3)	1.529	1.541
$C_{cluster}$–B2/3/4/5/6	1.706(6)	1.698	1.707		1.698	1.706
B–B (upper belt)	1.769(7)	1.773	1.780	1.702(5)	1.773	1.780
B–B (inter belt)	1.768(6)	1.766	1.771	–	1.767	1.773
B–B (lower belt)	1.787(6)	1.783	1.792	1.800(5)[c]	1.783	1.794
B12–B8/9/10/11/12	1.782(6)	1.780	1.792		1.782	1.797
Bond angles [°]						
B–C≡C (B12)	178.7(7)	180.00	180.00	177.3(1)	179.9	179.7
B–C≡C (B7)	–	–	–	177.3(1)	179.9	179.7

[a] (RI)-MP2/def2-TZVPP.
[b] B3LYP/6-311++G(d,p).
[c] The anion **2** is disordered over two positions; the crystallographic mirror plane is not consistent with the mirror plane in the calculated structure of the anion.

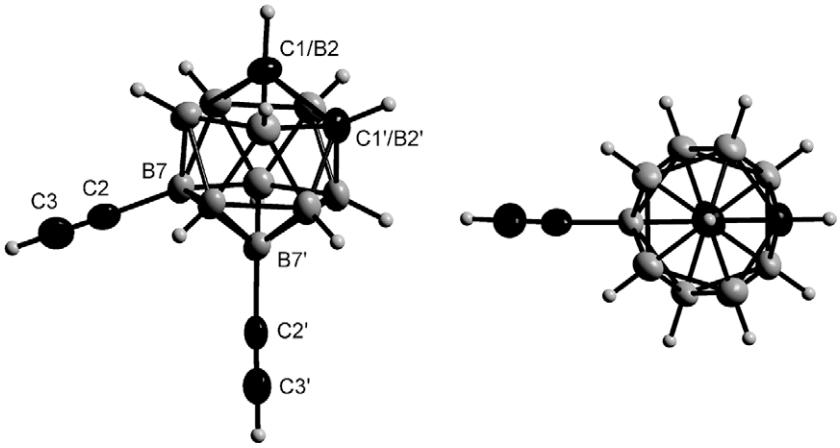

Fig. 2. Two different views of the disordered [7,12-$(HCC)_2$-*closo*-$CB_{11}H_{10}]^-$ anion in the crystal structure of $[Et_4N]$-**2** (displacement ellipsoids at the 40% probability level).

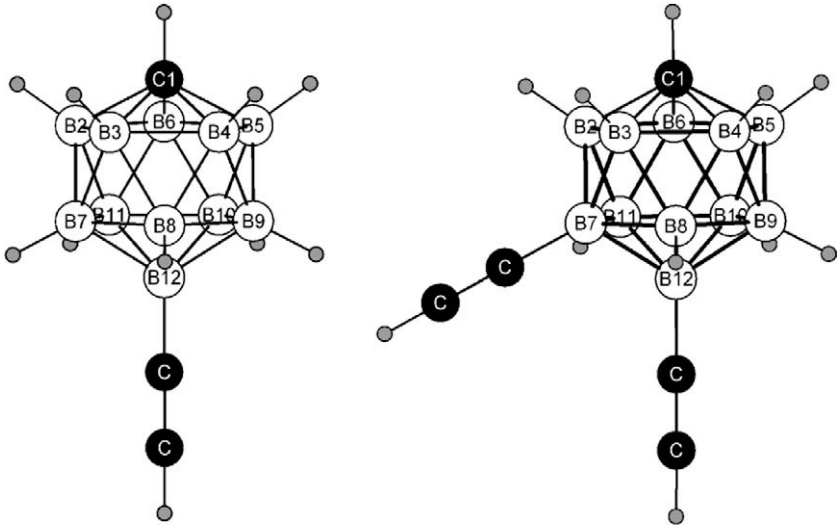

Fig. 3. Calculated structures of the [12-HCC-*closo*-$CB_{11}H_{11}]^-$ (**1**) and [7,12-$(HCC)_2$-*closo*-$CB_{11}H_{10}]^-$ (**2**) with labeling of the cluster atoms [(RI)-MP2/def2-TZVPP].

1.17(1) Å for **1** and *d*(B–C) = 1.548(2) Å and *d*(C≡C) = 1.202(2) Å for [12-PhCC-*closo*-1-$CB_{11}H_{11}]^-$. So far, structural analyses of boron clusters with ethynyl groups bonded to one of the boron atoms are rare; one further example is the cyclopentadienyliron tricarbonyl complex [1-(η^5-C_5H_5)-2-Ph-6-(HCC)-*closo*-1,2,3,4-$FeC_3B_7H_8$] [58]. The boron–carbon and carbon–carbon distances reported for the iron complex of 1.542(3) and 1.188(3) Å, respectively, are similar to the values determined for the [12-HCC-*closo*-1-$CB_{11}H_{11}]^-$ anion (**1**).

In the crystal of Cs-**1** the cesium cations and the [12-HCC-*closo*-1-$CB_{11}H_{11}]^-$ anions form infinite chains along the *b* axis (Fig. 4). The Cs···$C_{ethinyl}$ distances in the range of 3.602(9)–3.732(7) Å are indicative for coulomb interactions, since they are longer than the sum of the covalent radius of C(sp) (0.69(1) Å [59]) and the ionic radius of Cs^+ (1.67–1.88 Å [60]). In the cesium salt of the related [12-PhCC-*closo*-1-$CB_{11}H_{11}]^-$ anion similar distances have been observed with *d*(Cs···$C_{ethinyl}$) of 3.497(10)–3.567(8) Å [25], and for a few transition metal acetylide complexes with Cs^+ cations related Cs···$C_{ethinyl}$ contacts have been reported: $Cs[(C_5HMe_4)_2Ti(CCSiMe_3)_2]$ 3.423(6)–3.379(5) Å [61], $\{[(Me_3tacn)Cr(CCH)_3]_3Cs\}^+$ (Me_3tacn = *N*,*N*′,*N*′-triemthyl-1,4,7-triazacyclononane) 3.375(5)–3.394(5) Å [62], and $Cs_2[Cd(CCH)_4]$ 3.36(2)–3.50(2) Å [63].

3.3. NMR spectroscopy

The ethynylmonocarba-*closo*-dodecaborate anions [12-HCC-*closo*-1-$CB_{11}H_{11}]^-$ (**1**) and [7,12-$(HCC)_2$-*closo*-1-$CB_{11}H_{10}]^-$ (**2**) were studied by ^1H, ^{11}B, and ^{13}C NMR spectroscopy and the chemical shifts and coupling constants are collected in Table 3. The assignment of the ^{11}B and ^1H NMR signals is aided by $^{11}B\{1H\}$–$^1H\{11B\}$ 2D [64,65] and $^{11}B\{1H\}$–$^{11}B\{1H\}$ COSY [66,67] experiments as well as by theoretical studies performed at the GIAO/B3LYP-6-311++G(2d,p) level. The proton signals and the signals of the carbon atoms of the ethynyl groups in anion **2** were assigned to the respective H–C≡C group using two-dimensional (2D) gradient-enhanced heteronuclear multiple-quantum correlation (gHMQC) and 2D gradient enhanced heteronuclear multiple-bond correlation (gHMBC) spectroscopy and the assignment is in agreement with the order derived from GIAO-DFT calculations (Table 3). However, the assignment of the ^{13}C NMR signals of the ethynyl groups in **2** to the ^{11}B NMR signal of the corresponding boron atom given in Table 3 is solely based on calculated chemical shifts (GIAO-DFT).

In Fig. 5 the ^{11}B and $^{11}B\{1H\}$ NMR spectra of the anions **1** and **2** are shown and in Fig. 6 the $^{11}B\{1H\}$–$^{11}B\{1H\}$ correlation spectrum is depicted. For the monoethynyl substituted anion **1** three signals

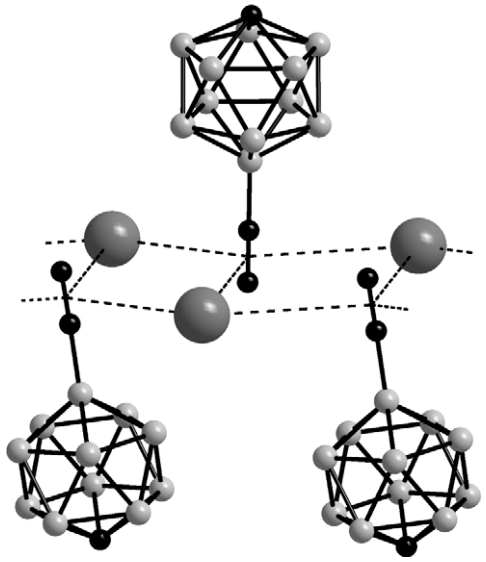

Fig. 4. A part of the chain formed by the [12-HCC-*closo*-$CB_{11}H_{11}$]$^-$ anions and the cesium cations in the crystal of Cs-**1** (the hydrogen atoms are omitted for clarity).

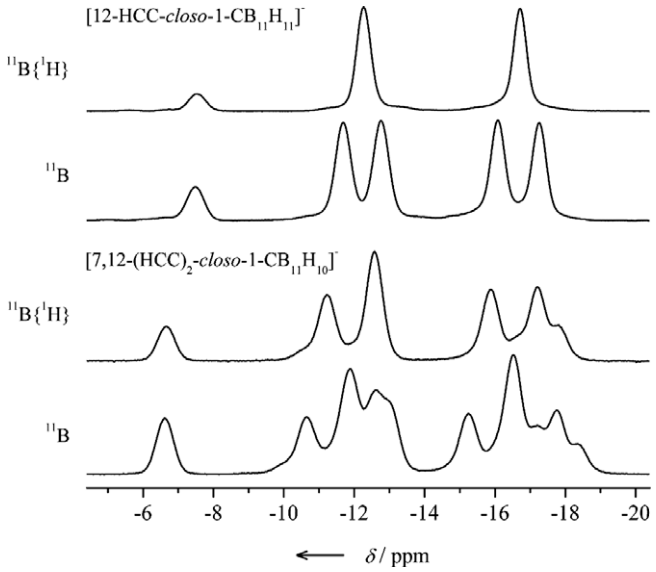

Fig. 5. ^{11}B and ^{11}B{1H} NMR spectra of [12-HCC-*closo*-$CB_{11}H_{11}$]$^-$ (**1**) and [7,12-$(HCC)_2$-*closo*-$CB_{11}H_{10}$]$^-$ (**2**).

Table 3
Experimental[a] and calculated[b] NMR spectroscopic data of [12-HCC-*closo*-1-$CB_{11}H_{11}$]$^-$ (**1**) and [7,12-$(HCC)_2$-*closo*-1-$CB_{11}H_{10}$]$^-$ (**2**).[c]

	[12-HCC-*closo*-1-$CB_{11}H_{11}$]$^-$ (**1**)		[7,12-$(HCC)_2$-*closo*-1-$CB_{11}H_{10}$]$^-$ (**2**)	
	Exp.[a]	Calc.[b]	Exp.[a]	Calc.[b]
$\delta(^{13}C)$ $C_{cluster}$	48.1	52.3	47.6	51.8
$\delta(^{13}C)$ B12–$^{13}C{\equiv}C$	96.0	104.2	94.6[d]	102.3
$\delta(^{13}C)$ B12–C$\equiv{}^{13}$C	80.9	74.5	82.1[d]	76.8
$\delta(^{13}C)$ B7–$^{13}C{\equiv}C$	–	–	93.4[d]	101.3
$\delta(^{13}C)$ B7–C$\equiv{}^{13}$C	–	–	80.9[d]	75.1
$\delta(^{11}B)$ B2+B3	−16.7[e]	−19.6	−15.9	−18.3
$\delta(^{11}B)$ B4+B6			−17.2	−20.1
$\delta(^{11}B)$ B5			−17.8	−21.0
$\delta(^{11}B)$ B7	−12.3[f]	−13.8	−12.6	−14.0
$\delta(^{11}B)$ B8+B11			−11.2	−11.9
$\delta(^{11}B)$ B9+B10			−12.6	−14.1
$\delta(^{11}B)$ B12	−7.5	−9.5	−6.7	−7.4
$\delta(^{1}H)$ $C_{cluster}$–^{1}H	2.17	1.83	2.22	1.87
$\delta(^{1}H)$ B12–C$\equiv$C–^{1}H	1.87	0.97	1.97	1.13
$\delta(^{1}H)$ B7–C$\equiv$C–^{1}H	–	–	1.95	1.04
$\delta(^{1}H)$ B2+B3	1.65	1.77	1.84	2.06
$\delta(^{1}H)$ B4+B6			1.62	1.82
$\delta(^{1}H)$ B5			1.56	1.73
$\delta(^{1}H)$ B8+B11	1.74	1.59	1.80	2.10
$\delta(^{1}H)$ B9+B10			1.70	2.03
$^{1}J(^{13}C,^{1}H)$ $^{13}C_{cluster}$–^{1}H	174.1	159.95	175.4	160.97
$^{1}J(^{13}C,^{1}H)$ B12–C$\equiv{}^{13}$C–^{1}H	234.3	228.64	234.0	229.61
$^{1}J(^{13}C,^{1}H)$ B7–C$\equiv{}^{13}$C–^{1}H	–	–	235.7	230.03
$^{2}J(^{13}C,^{1}H)$ B12–$^{13}C{\equiv}C$–^{1}H	45.4	43.80	46.0	44.13
$^{2}J(^{13}C,^{1}H)$ B7–$^{13}C{\equiv}C$–^{1}H	–	–	43.5	44.30
$^{1}J(^{13}C,^{11}B)$ ^{11}B12–$^{13}C{\equiv}C$	101.5[g]	105.41	103.1	107.28
$^{1}J(^{13}C,^{11}B)$ ^{11}B7–$^{13}C{\equiv}C$	–	–	104.1	108.40
$^{2}J(^{13}C,^{11}B)$ ^{11}B12–C$\equiv{}^{13}$C	19.1	21.76	19.0	21.88
$^{2}J(^{13}C,^{11}B)$ ^{11}B7–C$\equiv{}^{13}$C	–	–	18.8	22.04
$^{3}J(^{1}H,^{1}H)$ ^{1}H–$C_{cluster}$–B–^{1}H	3.4	3.59	3.4	3.6[h]
$^{3}J(^{11}B,^{1}H)$ ^{11}B12–C$\equiv$C–^{1}H	4[i]	3.51	4[i,j]	3.60
$^{3}J(^{11}B,^{1}H)$ ^{11}B7–C$\equiv$C–^{1}H	–	–	4[i,j]	3.64

[a] $[Et_4N]^+$ salts in $(CD_3)_2CO$.
[b] GIAO/B3LYP/6-311++G(2d,p) using geometries calculated at the B3LYP/6-311++G(d,p) level of theory.
[c] δ in ppm and J in Hz.
[d] The assignment of the position of the cluster is based on calculated chemical shifts.
[e] $^{1}J(^{11}B,^{1}H)$ = 151.0 Hz (calc.: 141.6 Hz).
[f] $^{1}J(^{11}B,^{1}H)$ = 137.8 Hz (calc.: 133.1 Hz).
[g] $^{1}\Delta^{13}C(^{10/11}B)$ = −0.0035 ppm.
[h] Mean value (3.56–3.66 Hz).
[i] Distorted quartet.
[j] Solvent: CD_3CN.

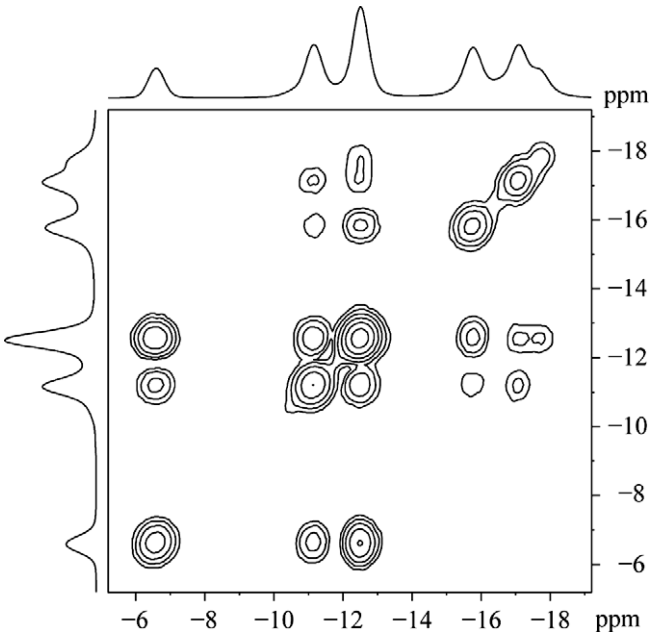

Fig. 6. $^{11}B\{1H\}$–$^{11}B\{1H\}$ COSY NMR spectrum of the [7,12-$(HCC)_2$-*closo*-$CB_{11}H_{10}]^-$ (**2**) anion.

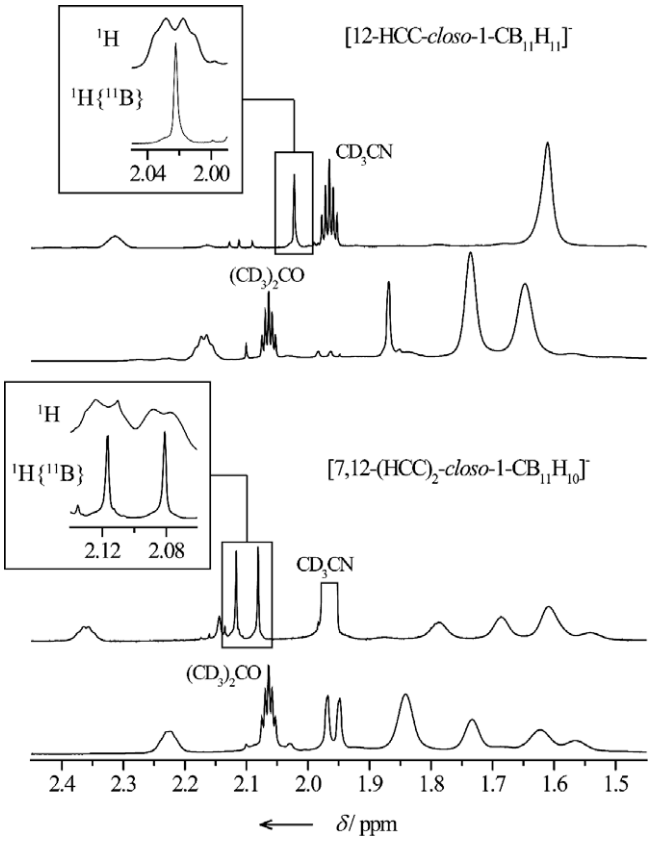

Fig. 7. $^1H\{11B\}$ NMR spectra of [12-HCC-*closo*-$CB_{11}H_{11}]^-$ (**1**) and [7,12-$(HCC)_2$-*closo*-$CB_{11}H_{10}]^-$ (**2**) in CD_3CN and $(CD_3)_2CO$ (in the grey boxes expanded sections of the ^1H and $^1H\{11B\}$ NMR spectra of the signals of the ethynyl protons are depicted).

with relative intensities of 1:5:5 corresponding to the three different boron positions of the {*closo*-CB_{11}} cluster that has C_{5v} symmetry are observed, and for the diethynyl substituted anion **2** that has C_s symmetry seven signals are detected. $\delta(^{11}B)$ observed for **1** and **2**

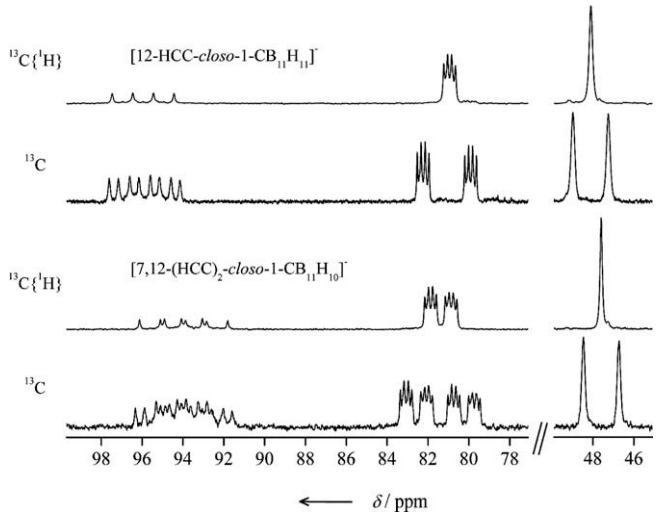

Fig. 8. $^{13}C\{1H\}$ and ^{13}C NMR spectra of [12-HCC-*closo*-$CB_{11}H_{11}]^-$ (**1**) and [7,12-$(HCC)_2$-*closo*-$CB_{11}H_{10}]^-$ (**2**) in CD_3CN and $(CD_3)_2CO$.

are close to the chemical shifts reported for related monocarba-*closo*-dodecaborate anions with trimethylsilyl- and phenylalkynyl substituents [25]. Some of the resonance frequencies of the ^{11}B nuclei of [12-HCC-*closo*-1-$CB_{11}H_{11}]^-$ (**1**) and [7,12-$(HCC)_2$-*closo*-1-$CB_{11}H_{10}]^-$ (**2**) show a significant solvent dependency: for example, $\delta(^{11}B)$ of **1** measured in CD_3CN solution are −8.0, −12.4, and −16.6 ppm for B12, B7–11, and B2–6, respectively, whereas in $(CD_3)_2CO$ different $\delta(^{11}B)$ of −7.5, −12.3, and −16.7 ppm are observed (Table 3). Hence, for the resonance frequency of the ^{11}B NMR signal corresponding to the antipodal boron atom that is bonded to the ethynyl group the strongest solvent dependency is found.

In the ^1H NMR spectra of [12-HCC-*closo*-1-$CB_{11}H_{11}]^-$ (**1**) and [7,12-$(HCC)_2$-*closo*-1-$CB_{11}H_{10}]^-$ (**2**) recorded in deutero-acetone and in deutero-acetonitrile a strong solvent dependency is observed as well, as evident from the $^1H\{11B\}$ NMR spectra presented in Fig. 7. For example, the ^1H NMR spectrum of **1** exhibits four signals in deutero-acetone and only three signals in deutero-acetonitrile. In the spectrum recorded in CD_3CN the two signals corresponding to the protons of the ten BH vertices are overlapped and shifted to 1.61 ppm from 1.65 and 1.77 ppm in $(CD_3)_2CO$. An even stronger solvent dependency is observed for $\delta(^1H)$ of the protons of the ethynyl groups and the CH-vertex in **1** and **2** (Fig. 7). The signals assigned to the protons of the CH fragments are split into sextets due to the coupling to the five protons of the upper B_5 belt. The sextet found in the spectrum of anion **2** is slightly distorted because of small differences in the three different $^3J(^1H,^1H)$ coupling constants (GIAO-DFT calculations, Table 3) that is a result of the lower symmetry of anion **2** (C_s) compared to anion **1** (C_{5v}).

In Fig. 7 enlarged plots of the $^1H\{11B\}$ and the ^1H NMR signals of the ethynyl proton in **1** and of both ethynyl protons in **2** are depicted. In the ^1H NMR spectra the signals are split into quartets due to the coupling to ^{11}B with $^3J(^{11}B,^1H) \approx 4$ Hz that is in excellent agreement to $^3J(^{11}B,^1H) = 3.51$–3.64 Hz derived from DFT calculations. The expected form of the signals with four lines of equal intensities and equal distances is not observed and distorted quartets are found. Partially collapsed signals are well known in NMR spectroscopy of boron compounds and they are a general phenomenon that occurs if a nucleus A couples to a nucleus B with spin > 1/2 and an inverse spin-lattice relaxation rate σ_1 that is close to the respective coupling constant $^nJ(A,B)$ [68–72]. In addition, the increased intensity of the two central lines of the quartets is to some extend due to the underlying partially collapsed septet of the corresponding ^{10}B isotopomer that has a relative intensity of 20%.

Table 4
Experimental[a] and calculated[b] vibrational data of [12-HCC-*closo*-1-$CB_{11}H_{11}$]$^-$ and [7,12-$(HCC)_2$-*closo*-1-$CB_{11}H_{10}$]$^-$.[c]

	[12-HCC-*closo*-1-$CB_{11}H_{11}$]$^-$ (**1**)		[7,12-$(HCC)_2$-*closo*-1-$CB_{11}H_{10}$]$^-$ (**2**)	
	Exp.[a]	Calc.[b]	Exp.[a]	Calc.[b]
$\tilde{\nu}$(C≡C)	2055	2145	2064	2150[d]/2152[e]
$\tilde{\nu}$($C_{C\equiv C}$–H)	3272	3474	3278/3264	3474.5/3474.7
$\tilde{\nu}$($C_{cluster}$–H)	3056	3193	3063	3196
$\tilde{\nu}$(B–H)	2593 – 2526	2649 – 2611	2590 – 2508	2658 – 2619

[a] Cs^+ salts.
[b] B3LYP/6-311++G(d,p).
[c] Wavenumbers in cm^{-1}.
[d] $\tilde{\nu}$(C≡C) of the ethynyl group bonded to B12.
[e] $\tilde{\nu}$(C≡C) of the ethynyl group bonded to B7.

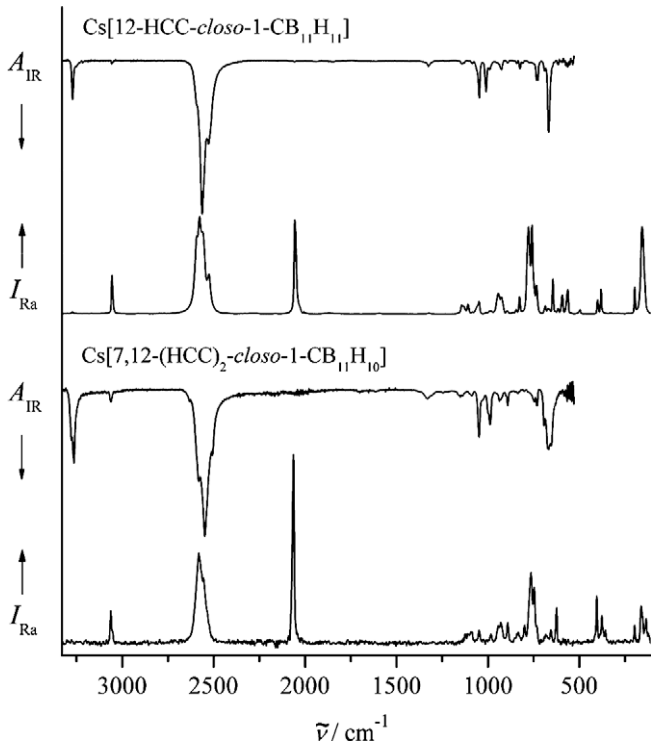

Fig. 9. The IR and Raman spectra of Cs[12-HCC-*closo*-$CB_{11}H_{11}$] (Cs-**1**) (top) and Cs[7,12-$(HCC)_2$-*closo*-$CB_{11}H_{10}$] (Cs-**2**) (bottom).

The $^{13}C\{1H\}$ and ^{13}C NMR spectra of [12-HCC-*closo*-1-$CB_{11}H_{11}$]$^-$ (**1**) and [7,12-$(HCC)_2$-*closo*-1-$CB_{11}H_{10}$]$^-$ (**2**) exhibit three and five signals corresponding to the cluster carbon atom and the carbon atoms of the ethynyl groups, respectively (Fig. 8 and Table 3). The signals of the cluster carbon atoms at approximately 48 ppm are singlets in the $^{13}C\{1H\}$ NMR spectra and doublets in the ^{13}C NMR spectra ($^1J(^{13}C,^1H)$ = 174.1 and 175.4 Hz). In the $^{13}C\{1H\}$ NMR spectra the signals corresponding to the ethynyl carbon atoms are split into quartets with lines of equal intensity. The one-bond ^{13}C–^{11}B coupling constants are in the range of 234.0–235.7 Hz and $^2J(^{13}C,^{11}B)$ vary from 18.8 to 19.1 Hz (Table 3). In the proton coupled ^{13}C NMR spectra the signals are further split into doublets due to the interaction with the terminal protons.

3.4. Vibrational spectroscopy

The cesium salts Cs[12-HCC-*closo*-1-$CB_{11}H_{11}$] (**1**) and Cs[7,12-$(HCC)_2$-*closo*-1-$CB_{11}H_{10}$] (**2**) were studied by IR and Raman spectroscopy and in Table 4 selected experimental band positions are compared to calculated wavenumbers (DFT). The strongest bands in the four spectra in Fig. 9 are assigned to $\tilde{\nu}$(B–H) (**1**: 2526–2593 cm^{-1}; **2**: 2508–2590 cm^{-1}). In the IR and Raman spectra $\tilde{\nu}$($C_{cluster}$–H) are observed at 3056 (**1**) and 3063 cm^{-1} (**2**). The values for $\tilde{\nu}$(B–H) and $\tilde{\nu}$($C_{cluster}$–H) are similar to band positions reported for the cesium salt of the parent anion [*closo*-1-$CB_{11}H_{12}$]$^-$ [73]. The carbon–carbon triple bond stretch results in a strong band in the Raman spectra of the anions **1** and **2** at 2055 and 2064 cm^{-1}, respectively. The two $\tilde{\nu}$(C≡C) in the diethynyl substituted anion **2** are not resolved. In contrast, $\tilde{\nu}$($C_{C\equiv C}$–H) that is observed in the IR spectra is split into two partial overlapping bands in the spectrum of Cs-**2** at 3264 and 3278 cm^{-1} and in the spectrum of Cs-**1** at 3272 cm^{-1}. For the related iron complex [1-(η^5-C_5H_5)-2-Ph-6-(HCC)-*closo*-1,2,3,4-$FeC_3B_7H_8$] IR spectroscopic data are available [58], and $\tilde{\nu}$(C≡C) as well as $\tilde{\nu}$($C_{C\equiv C}$–H) can be assigned to 2068 and 3272 cm^{-1}, respectively, similar to the values observed for anions **1** and **2**.

4. Conclusions

Salts of monocarba-*closo*-dodecaborate anions with one and two terminal alkynyl groups bonded to the boron atoms in the 7 and 12 position of the cluster are now available in three, straight forward steps starting from commercially available Cs[*closo*-1-$CB_{11}H_{12}$] [25,32]. The anions [12-HCC-*closo*-1-$CB_{11}H_{11}$]$^-$ (**1**) and [7,12-$(HCC)_2$-*closo*-1-$CB_{11}H_{10}$]$^-$ (**2**) described in this contribution are among the rare examples of {*closo*-1-CB_{11}} derivatives with functional groups bonded to the boron atoms of the 12-vertex cluster that, in principle, can be easily modified [1,74], and thus may lead to new applications for compounds containing a {*closo*-1-CB_{11}} cluster. For example, the ethynyl substituted anions **1** and **2** are promising ligands for coordination chemistry, as evident from a comparison to the related dicarba-*closo*-dodecaboranes with ethynyl groups bonded to the cluster carbon atoms that have been used for the preparation of a variety of transition metal complexes [75–78].

Acknowledgements

Financial support by the Fonds der Chemischen Industrie (FCI) is gratefully acknowledged. Furthermore, the authors are grateful to Merck KGaA, Darmstadt (Germany) for chemicals used. The authors thank Professor W. Frank for generous support and helpful discussions, and Dr. G.J. Reiss, Mr. J.A.P. Sprenger, Mrs. E. Hammes, and Mr. P. Roloff, for technical support.

Appendix A. Supplementary material

CCDC 752149 and 752148 contain the supplementary crystallographic data for Cs-**1** and [Et_4N]-**2**, respectively. These data can be obtained free of charge from The Cambridge Crystallographic Data Centre via www.ccdc.cam.ac.uk/data_request/cif. Supplementary

data associated with this article can be found, in the online version, at doi:10.1016/j.jorganchem.2010.02.011.

References

[1] S. Körbe, P.J. Schreiber, J. Michl, Chem. Rev. 106 (2006) 5208–5249.
[2] P. Kaszynski, Collect. Czech. Chem. Commun. 64 (1999) 895–926.
[3] J. Michl, Pure Appl. Chem. 80 (2008) 429–446.
[4] Y. Zhang, K. Huynh, I. Manners, C.A. Reed, Chem. Commun. (2008) 494–496.
[5] C.A. Reed, Acc. Chem. Res. 43 (2010) 121–128.
[6] A.S. Larsen, J.D. Holbrey, F.S. Tham, C.A. Reed, J. Am. Chem. Soc. 122 (2000) 7264–7272.
[7] Y.H. Zhu, C.B. Ching, K. Carpenter, R. Xu, S. Selvaratnam, N.S. Hosmane, J.A. Maguire, Appl. Organomet. Chem. 17 (2003) 346–350.
[8] D.J. Crowther, S.L. Borkowsky, D. Swenson, T.Y. Meyer, R.F. Jordan, Organometallics 12 (1993) 2897–2903.
[9] S. Moss, B.T. King, A. de Meijere, S.I. Kozhushkov, P.E. Eaton, J. Michl, Org. Lett. 3 (2001) 2375–2377.
[10] S.H. Strauss, S.V. Ivanov, Colorado State University Research Foundation, WO 02/36557/A2, 2002.
[11] N.J. Patmore, C. Hague, J.H. Cotgreave, M.F. Mahon, C.G. Frost, A.S. Weller, Chem. Eur. J. 8 (2002) 2088–2098.
[12] K.-C. Kim, C.A. Reed, G.S. Long, A. Sen, J. Am. Chem. Soc. 124 (2002) 7662–7663.
[13] C. Douvris, O.V. Ozerov, Science 321 (2008) 1188–1190.
[14] W. Gu, M.R. Haneline, C. Douvris, O.V. Ozerov, J. Am. Chem. Soc. 131 (2009) 11203–11212.
[15] K. Vyakaranam, J.B. Barbour, J. Michl, J. Am. Chem. Soc. 131 (2009) 3132–3133.
[16] D.S. Wilbur, D.K. Hamlin, R.R. Srivastava, M.K. Chyan, Nucl. Med. Biol. 31 (2004) 523–530.
[17] V.A. Ol'shevskaya, A.V. Zaitsev, V.N. Luzgina, T.T. Kondratieva, O.G. Ivanov, E.G. Kononova, P.V. Petrovskii, A.F. Mironov, V.N. Kalinin, J. Hofmann, A.A. Shtil, Bioorg. Med. Chem. 14 (2006) 109–120.
[18] Y. Qin, E. Bakker, Anal. Chem. 75 (2003) 6002–6010.
[19] K. Vyakaranam, S. Körbe, J. Michl, J. Am. Chem. Soc. 128 (2006) 5680–5686.
[20] B. Grüner, Z. Janoušek, B.T. King, J.N. Woodford, C.H. Wang, V. Všetečka, J. Michl, J. Am. Chem. Soc. 121 (1999) 3122–3126.
[21] A. Franken, C.A. Kilner, M. Thornton-Pett, J.D. Kennedy, J. Organomet. Chem. 657 (2002) 176–179.
[22] N.J. Bullen, A. Franken, C.A. Kilner, J.D. Kennedy, Chem. Commun. (2003) 1684–1685.
[23] J.H. Morris, K.W. Henderson, V.A. Ol'shevskaya, J. Chem. Soc., Dalton Trans. (1998) 1951–1959.
[24] A. Franken, C.A. Kilner, M. Thornton-Pett, J.D. Kennedy, Collect. Czech. Chem. Commun. 67 (2002) 869–912.
[25] M. Finze, Inorg. Chem. 47 (2008) 11857–11867.
[26] L.I. Zakharkin, A.I. Kovredov, V.A. Ol'shevskaya, Russ. J. Gen. Chem. 51 (1981) 2422.
[27] L.I. Zakharkin, A.I. Kovredov, V.A. Ol'shevskaya, Russ. Chem. Bull. 30 (1981) 1775–1777.
[28] L.I. Zakharkin, A.I. Kovredov, V.A. Ol'shevskaya, Z.S. Shaugumbekova, J. Organomet. Chem. 226 (1982) 217–222.
[29] M. Kumada, K. Tamao, K. Sumitani, J. Am. Chem. Soc. 94 (1972) 4374–4376.
[30] K. Tamao, K. Sumitani, Y. Kiso, M. Zembayashi, A. Fujioka, S. Kodama, I. Nakajima, A. Minato, M. Kumada, Bull. Chem. Soc. Jpn. 49 (1976) 1958–1969.
[31] T. Jelínek, J. Plešek, S. Heřmánek, B. Štíbr, Collect. Czech. Chem. Commun. 51 (1986) 819–829.
[32] M. Finze, Eur. J. Inorg. Chem. (2009) 501–507.
[33] X-RED 1.20, Stoe Data Reduction Program, STOE & Cie GmbH, Darmstadt, Germany, 2000.
[34] X-SHAPE 1.06, Crystal Optimization for Numerical Absorption Correction, STOE & Cie GmbH, Darmstadt, Germany, 1999.
[35] G.M. Sheldrick, SHELXS-97, Program for Crystal Structure Solution, Universität Göttingen, 1997.
[36] G.M. Sheldrick, Acta Crystallogr., Sect. A 64 (2008) 112–122.
[37] G.M. Sheldrick, SHELXL-97, Program for Crystal Structure Refinement, Universität Göttingen, 1997.
[38] S. Paavola, F. Teixidor, C. Viñas, R. Kivekäs, J. Organomet. Chem. 657 (2002) 187–193.
[39] L.J. Farrugia, J. Appl. Crystallogr. 32 (1999) 837–838.
[40] K. Brandenburg, DIAMOND 3.2c, Crystal Impact GbR, Bonn, Germany, 2006.
[41] W. Kohn, L.J. Sham, Phys. Rev. A 140 (1965) 1133.
[42] A.D. Becke, Phys. Rev. B: Condens. Matter 38 (1988) 3098–3100.
[43] A.D. Becke, J. Chem. Phys. 98 (1993) 5648.
[44] C. Lee, W. Yang, R.G. Parr, Phys. Rev. B: Condens. Matter 41 (1988) 785.
[45] M.J. Frisch, G.W. Trucks, H.B. Schlegel, G.E. Scuseria, M.A. Robb, J.R. Cheeseman, J.A. Montgomery Jr., T. Vrene, K.N. Kudin, J.C. Burant, J.M. Millam, S.S. Iyengar, J. Tomasi, V. Barone, B. Mennucci, M. Cossi, G. Scalmani, N. Rega, G.A. Petersson, H. Nakatsuji, M. Hada, M. Ehara, K. Toyota, R. Fukuda, J. Hasegawa, M. Ishida, T. Nakajima, Y. Honda, O. Kitao, H. Nakai, M. Klene, X. Li, J.E. Knox, H.P. Hratchian, J.B. Cross, V. Bakken, C. Adamo, J. Jaramillo, R. Gomperts, R.E. Stratmann, O. Yazyev, A.J. Austin, R. Cammi, C. Pomelli, J.W. Ochterski, P.Y. Ayala, K. Morokuma, G.A. Voth, P. Salvador, J.J. Dannenberg, V.G. Zakrzewski, S. Dapprich, A.D. Daniels, M.C. Strain, O. Farkas, D.K. Malick, A.D. Rabuck, K. Raghavachari, J.B. Foresman, J.V. Ortiz, Q. Cui, A.G. Baboul, S. Clifford, J. Cioslowski, B.B. Stefanov, G. Liu, A. Liashenko, P. Piskorz, I. Komaromi, R.L. Martin, D.J. Fox, T. Keith, M.A. Al-Laham, C.Y. Peng, A. Nanayakkara, M. Challacombe, P.M.W. Gill, B. Johnson, W. Chen, M.W. Wong, C. Gonzalez, J.A. Pople, GAUSSIAN 03, Revision D.01, Gaussian, Inc., USA, 2004.
[46] J.C. Rienstra-Kiracofe, G.S. Tschumper, H.F. Schaefer III, S. Nandi, G.B. Ellison, Chem. Rev. 102 (2002) 231.
[47] C. Hättig, F. Weigend, J. Chem. Phys. 113 (2000) 5154–5161.
[48] The Corresponding Literature for the Basis Sets can be Found at: <ftp://ftp.chemie.uni-karlsruhe.de/pub/basen>.
[49] K. Wolinski, J.F. Hinton, P. Pulay, J. Am. Chem. Soc. 112 (1990) 8251.
[50] T. Helgaker, M. Watson, N.C. Handy, J. Chem. Phys. 113 (2000) 9402–9409.
[51] V. Sychrovsky, J. Grafenstein, D. Cremer, J. Chem. Phys. 113 (2000) 3530–3547.
[52] V. Barone, J.E. Peralta, R.H. Contreras, J.P. Snyder, J. Phys. Chem. A 106 (2002) 5607–5612.
[53] J.E. Peralta, G.E. Scuseria, J.R. Cheeseman, M.J. Frisch, Chem. Phys. Lett. 375 (2003) 452–458.
[54] J.D. Kennedy, in: J. Mason (Ed.), Multinuclear NMR, Plenum Press, New York, 1987, p. 221.
[55] S. Berger, S. Braun, H.-O. Kalinowski, NMR-Spektroskopie von Nichtmetallen - ^{19}F-NMR-Spektroskopie, Vol. 4, Georg Thieme Verlag, Stuttgart, 1994.
[56] A.G. Douglass, Z. Janousek, P. Kaszynski, Inorg. Chem. 37 (1998) 6361–6365.
[57] M. Finze, G.J. Reiss, Acta Crystallogr., Sect. E 65 (2009) o1048.
[58] R. Butterick III, P.J. Carroll, L.G. Sneddon, Organometallics 27 (2008) 4419–4427.
[59] B. Cordero, V. Gomez, A.E. Platero-Prats, M. Reves, J. Echeverria, E. Cremades, F. Barragan, S. Alvarez, Dalton Trans. (2008) 2832–2838.
[60] R.D. Shannon, Acta Crystallogr., Sect. A 32 (1976) 751–767.
[61] J. Hiller, V. Varga, U. Thewalt, K. Mach, Collect. Czech. Chem. Commun. 62 (1997) 1446–1456.
[62] L.A. Berben, J.R. Long, J. Am. Chem. Soc. 124 (2002) 11588–11589.
[63] U. Cremer, U. Ruschewitz, Z. Anorg. Allg. Chem. 630 (2004) 337–343.
[64] D.C. Finster, W.C. Hutton, R.N. Grimes, J. Am. Chem. Soc. 102 (1980) 400–401.
[65] I.J. Colquhoun, W. McFarlane, J. Chem. Soc., Dalton Trans. (1981) 2014–2016.
[66] T.L. Venable, W.C. Hutton, R.N. Grimes, J. Am. Chem. Soc. 104 (1982) 4716–4717.
[67] T.L. Venable, W.C. Hutton, R.N. Grimes, J. Am. Chem. Soc. 106 (1984) 29–37.
[68] T.K. Halstead, P.A. Osment, B.C. Sanctuary, J. Tangenfeldt, I.J. Lowe, J. Magn. Reson. 67 (1986) 267–306.
[69] B. Wrackmeyer, in: G.A. Webb (Ed.), Annu. Rep. NMR Spectrosc., vol. 20, Academic Press, Limited, London, UK, 1988, pp. 61–203.
[70] A. Abragam, Principles of Nuclear Magnetism, Clarendon Press, Oxford, UK, 1986.
[71] M. Finze, E. Bernhardt, A. Terheiden, M. Berkei, H. Willner, D. Christen, H. Oberhammer, F. Aubke, J. Am. Chem. Soc. 124 (2002) 15385–15398.
[72] M. Finze, E. Bernhardt, H. Willner, C.W. Lehmann, J. Am. Chem. Soc. 127 (2005) 10712–10722.
[73] E.G. Kononova, S.S. Bukalov, L.A. Leites, K.A. Lyssenko, V.A. Ol'shevskaya, Russ. Chem. Bull., Int. Ed. 52 (2003) 85–92.
[74] M. Finze, Chem. Eur. J. 15 (2009) 947–962.
[75] L.I. Zakharkin, A.I. Kovredov, V.A. Ol'shevskaya, Russ. Chem. Bull. 31 (1982) 599–602.
[76] T.J. Wedge, A. Herzog, R. Huertas, M.W. Lee, C.B. Knobler, M.F. Hawthorne, Organometallics 23 (2004) 482–489.
[77] H. Jude, H. Disteldorf, S. Fischer, T. Wedge, A.M. Hawkridge, A.M. Arif, M.F. Hawthorne, D.C. Muddiman, P.J. Stang, J. Am. Chem. Soc. 127 (2005) 12131–12139.
[78] M.A. Fox, R.L. Roberts, T.E. Baines, B. Le Guennic, J.-F. Halet, F. Hartl, D.S. Yufit, D. Albesa-Jové, J.A.K. Howard, P.J. Low, J. Am. Chem. Soc. 130 (2008) 3566–3578.